

1 **Enhancing a multi-purpose artificial urine for culture and gene expression studies of**
2 **uropathogenic *Escherichia coli* strains**

3 Patricia T. Rimbi¹, Nicky O'Boyle², Gillian R. Douce¹, Mariagrazia Pizza³, Roberto Rosini⁴,
4 Andrew J. Roe^{1*}

5 ¹ School of Infection and Immunity, University of Glasgow, Glasgow, G12 8TA, United
6 Kingdom

7 ² School of Microbiology, University College Cork, National University of Ireland, Cork, T12
8 K8AF, Ireland

9 ³ Centre for Bacterial Resistance Biology, Imperial College London, London, SW7 2AZ, United
10 Kingdom

11 ⁴ GSK Vaccines, Siena, Italy

12 ***Corresponding author:** Professor Andrew Roe. Address: B214, Sir Graeme Davies Building,
13 120 University Place, Glasgow, G12 8TA, United Kingdom. Email:
14 andrew.roe@glasgow.ac.uk

15 **Running title:** Enhanced artificial urine

16

17 **Abstract**

18 **Aims:** The main objective of this study was to modify a recently reported multi-purpose
19 artificial urine (MP-AU) for culture and gene expression studies of uropathogenic *Escherichia*
20 *coli* (UPEC) strains.

21 **Methods and results:** We used liquid chromatography mass spectrometry (LC-MS) to
22 identify and adjust the metabolic profile of MP-AU closer to that of pooled human urine
23 (PHU). Modification in this way facilitated growth of UPEC strains with growth rates similar
24 to those obtained in PHU. Transcriptomic analysis of UPEC strains cultured in enhanced
25 artificial urine (enhanced AU) and PHU showed that the gene expression profiles are similar,
26 with less than 7% of genes differentially expressed between the two conditions.

27 **Conclusions:** Enhancing an MP-AU with metabolites identified in PHU allows the enhanced
28 AU to be used as a substitute for the culture and *in vitro* gene expression studies of UPEC
29 strains.

30 **Impact statement:** The data support this enhanced AU as a robust medium to study aspects
31 of UPEC physiology *in vitro*.

32 **Keywords:** artificial urine, uropathogen, *E. coli*, transcriptome

33

34 **Materials and methods**

35 *Bacterial growth conditions*

36 All strains (Table 1) were cultured in lysogeny broth (LB) medium overnight at 37°C, 200
37 rpm. UPEC strains CFT073 and UTI89 were isolated from the blood of patients with
38 pyelonephritis (Mobley *et al.*, 1990) and cystitis (Hultgren *et al.*, 1986), respectively. The EC0
39 and EC1 bacteremia isolates were a gift from Professor Thomas Evans' laboratory and were
40 isolated from the blood of hospitalized patients as described elsewhere (Goswami *et al.*,
41 2018). For growth assays and growth for transcriptomic analysis, overnight cultures were
42 diluted in culture medium (pooled human urine (PHU), MP-AU or enhanced AU), pre-
43 warmed to 37°C, to an OD600 of 0.06. Cultures were incubated at 37°C, 200 rpm for 8 h
44 growth assays, or until the desired OD600 was reached for RNA extraction and subsequent
45 transcriptomic analysis. For growth assays, the optical density of 1 mL neat samples was
46 measured at hourly intervals.

47 *Pooled human urine (PHU)*

48 The first morning urine from five healthy volunteers was pooled and filtered using a 0.22 µm
49 vacuum filter (Sigma). Here, healthy describes the absence of infection. Volunteers were not
50 asked to disclose other factors such as gender, diet, medication, or menstruation status.
51 PHU was stored at 4°C for use within four days or aliquoted and stored at -20°C for later
52 use. Frozen aliquots were thawed at 4°C overnight and brought to room temperature before
53 use.

54 *Multi-purpose artificial urine (MP-AU)*

55 MP-AU was adapted from the literature (Sarigul *et al.*, 2019). All components except uric
56 acid were prepared as 1 mol L⁻¹ or 0.5 mol L⁻¹ stock solutions in distilled deionized water and
57 filter sterilized (Table 2). Uric acid was added in powder form as it is not easily dissolved in

58 water. 1 mol L⁻¹ urea was prepared on the day of use. In general, MP-AU without urea was
59 prepared the day before use.

60 *Enhanced AU*

61 Supplement solutions were prepared in water and filter sterilized, with the exception of L-
62 tyrosine, which was mixed in water but not filtered, due to its insolubility in water (Table
63 S1). Supplements were added to MP-AU, with urea, at a final concentration of 5 mmol L⁻¹ on
64 the day of use.

65 *Transcriptomic analysis*

66 To directly compare the transcriptomic profile of UPEC strain CFT073 in MP-AU and PHU,
67 CFT073 was cultured in triplicate in M9 minimal medium for 4 h. Cells were pelleted down
68 by centrifugation at 2907 × *g* for 5 mins and resuspended in MP-AU or PHU. After 1 h
69 culture in MP-AU or PHU, samples were taken and normalized to OD600 ~0.6. To compare
70 the transcriptomic profile of CFT073 and UTI89 in enhanced AU and PHU, UPEC strains
71 CFT073 and UTI89 were cultured in triplicate in enhanced AU or PHU until OD600 of >0.4
72 (mid-exponential phase). Cultures were normalized to OD600 1.0. For all transcriptomic
73 analysis experiments, cells were centrifuged at 10000 × *g* for 1 min and the pellet was
74 resuspended in RNeasy Protect Bacteria Reagent (Qiagen). The cells were incubated at room
75 temperature for 10 mins and centrifuged as before. The supernatant was aspirated and the
76 pellet was stored at -20°C until RNA extraction within four days. Total RNA was isolated as
77 per manufacturer's instructions using the PureLink RNA Mini Kit (Invitrogen). DNA was
78 removed using TURBO DNase (Invitrogen). RNA was further extracted using
79 phenol:chloroform:isoamyl alcohol (Invitrogen) and was precipitated using 100% ethanol
80 (Fisher Scientific). The concentration and purity of the extracted RNA was quantified using a
81 spectrophotometer (DeNovix). The integrity of RNA was assessed by running gel

82 electrophoresis to examine 23S and 16S rRNA bands. The presence of residual or
83 contaminant DNA was determined by polymerase chain reaction to amplify *fimA*. Samples
84 were sent to Glasgow Polyomics for ribosomal depletion using a QIAseq FastSelect
85 5S/16S/23S Kit (Qiagen). A cDNA library was prepared using a TruSeq Stranded Total RNA
86 Library Prep Gold kit (Illumina). RNA sequencing was performed to a depth of 10 million 75
87 bp or 100 bp single end reads using a NextSeq500 or NextSeq2000 sequencing system
88 (Illumina). Data were analyzed using CLC Genomics Workbench version 21.0.5 (Qiagen).
89 Reads were mapped to the CFT073 and UTI89 reference genomes (NCBI accession numbers
90 NC_004431.1 and NC_007946.1, respectively) using default parameters. Differential
91 expression was calculated using the Differential Expression for RNA-seq tool in CLC
92 Genomics Workbench. Genes were taken as significantly differentially expressed with a fold
93 change of ≥ 1.5 or ≤ -1.5 and a false-discovery rate (FDR)-corrected *P* value of ≤ 0.05 . Volcano
94 plots were generated using Prism version 9.5.1 (GraphPad). Functional categories of the
95 differentially expressed genes (DEGs) were assigned using the UniProtKB gene ontology
96 (GO) biological process annotation in the first instance, or the GO molecular function where
97 the GO biological process annotation was not available (Bateman *et al.*, 2021). Raw
98 sequencing data have been deposited in the European Nucleotide Archive under the project
99 accession number PRJEB55151.

100 *Metabolomics analysis*

101 Metabolites were extracted from PHU or MP-AU using an extraction solvent of
102 chloroform:methanol:water in a 1:3:1 v/v/v ratio. The components for the extraction
103 solvent were all high-performance liquid chromatography (HPLC) grade and supplied by
104 Fisher Scientific. Extracted metabolites were analyzed by LC-MS by Glasgow Polyomics using
105 a Dionex UltiMate 3000 RSLC system and an Q Exactive Orbitrap (Thermo Fisher Scientific).

106 Data were analyzed using the Glasgow Polyomics Integrated Metabolomics Pipeline (PiMP)
107 software (Gloaguen *et al.*, 2017). Statistical analysis, the Venn diagram and bar charts were
108 generated using Prism version 9.5.1 (GraphPad).

109 *Iron quantification*

110 ICP-MS of acidified PHU, MP-AU and enhanced AU containing final concentration 1 mmol L⁻¹
111 iron (II) sulfate heptahydrate (Sigma-Aldrich) was performed by Dr Lorna Eades at the
112 University of Edinburgh using the 8900 Triple Quadrupole ICP-MS instrument (Agilent). The
113 samples were acidified with trace metal grade nitric acid (Fisher Scientific) and analytical
114 reagent grade hydrochloric acid (Fisher Scientific).

115

116

117 **Introduction**

118 Uropathogenic *Escherichia coli* (UPEC) strains are the leading cause of urinary tract
119 infections, which have associated morbidities, mortality, and economic burden. UPEC strains
120 disseminate from the gastrointestinal tract and colonize the periurethral area, from which
121 they can invade and colonize the urinary tract. Hence, urine is arguably the most
122 appropriate growth medium to culture UPEC *in vitro* and for studying gene expression,
123 however there are many hurdles associated with the use of urine. These challenges include
124 variations in composition (Sarigul *et al.*, 2019), the need for donors, and the stability of urine
125 over time. Therefore, to better understand UPEC physiology *in vitro* we need a growth
126 medium that is physiologically relevant and highly reproducible. Artificial urine has been
127 used for different purposes in the literature, for example to examine the expression of
128 virulence genes in UPEC strain CFT073 during cell adhesion (Sarshar *et al.*, 2022). Certain

129 formulations have components that are not normally found in healthy human urine, such as
130 bicarbonate (Brooks and Keevil, 1997) and therefore are not the most accurate
131 representation of the chemical profile of healthy human urine.

132 Analytical techniques such as mass spectrometry, nuclear magnetic resonance, and liquid
133 chromatography mass spectrometry (LC-MS) have been combined to demonstrate that
134 human urine is a complex medium, with thousands of components (Sarigul *et al.*, 2019).

135 Based on this analysis, a recent publication formulated an artificial urine that tried to
136 replicate healthy human urine (Sarigul *et al.*, 2019). The authors compared their multi-
137 purpose artificial urine (MP-AU) to urine collected from 28 individuals by using attenuated
138 total reflection-Fourier transform infrared spectroscopy (Sarigul *et al.*, 2019). The 13
139 components of MP-AU were shown to be at more physiologically relevant levels compared
140 to the two other artificial urine formulations (Brooks and Keevil, 1997; Chutipongtanate and
141 Thongboonkerd, 2010; Sarigul *et al.*, 2019). In this study, we aimed to determine whether
142 Sarigul's MP-AU could be used as an alternative to human urine in *in vitro* studies of UPEC
143 strains. We have taken the pre-existing MP-AU and enhanced it with specific metabolites
144 present in human urine to support the growth of UPEC strains *in vitro*.

ORIGINAL UNEDITED MANUSCRIPT

145 **Results**

146 *MP-AU does not support the growth of UPEC strains in vitro*

147 To determine whether MP-AU is suitable for the culture of UPEC strains *in vitro*, we
148 performed growth assays of prototypic UPEC strains CFT073 and UTI89 in this medium. The
149 growth rates of these strains in MP-AU were compared to those obtained for growth in
150 PHU. Sarigul's MP-AU did not support the optimal growth of UPEC strains CFT073 or UTI89
151 (Fig. 1a). The optical density of CFT073 and UTI89 in MP-AU decreased in the first hour of
152 growth, suggesting that there was some lysis of the bacterial cells. Sarigul *et al.* suggests
153 adding peptone and yeast extract to MP-AU for bacterial growth studies (Sarigul *et al.*,
154 2019), however, these were omitted here due to their absence in healthy human urine and
155 subsequent unsuitability for gene expression studies against PHU. To allow for
156 transcriptomic analysis of CFT073 in MP-AU or PHU, bacteria were first cultured in M9
157 minimal medium before being resuspended in either MP-AU or PHU (Fig. 1b). There were
158 vast differences in the transcriptomic profile following 1 h exposure to MP-AU or PHU, with
159 3284 differentially expressed genes in MP-AU compared to PHU (Fig. 1c). This corresponds
160 to a shift in 66.9% of the CFT073 coding sequences. 1607 of these genes were upregulated,
161 while 1677 were downregulated. The ten most significantly upregulated genes include those
162 involved in arginine catabolism and carboxylic acid catabolism (*astABCDE*, *fadB*), as well as
163 *argT*, which encodes a lysine/arginine/ornithine ABC transporter substrate-binding protein,
164 *C_RS19130* (previously *c4034* or *yhdW*), and *yhdX* and *ytfT*, which encode ABC transporter
165 permeases. The ten most significantly downregulated genes include *glnA*, *cyuA*, *gcvT*, *gcvH*,
166 *lacY*, *rplC*, *lacA*, *rplD*, *sitC*, and *chuY*.

167 *Metabolomic analysis of PHU*

168 Sarigul *et al.* demonstrated that the levels of components in their MP-AU are similar to
169 healthy human urine (Sarigul *et al.*, 2019). However, as the MP-AU did not facilitate the
170 growth of UPEC strains *in vitro*, we hypothesized that there were components in healthy
171 human urine that could be used to supplement MP-AU and support the growth of UPEC
172 strains. LC-MS analysis was used to identify and compare the relative abundance of
173 metabolites extracted from MP-AU and healthy human urine samples. Untargeted LC-MS
174 identified 68 metabolites across all samples and putatively annotated a further 5703
175 metabolites, however as many of these shared a peak ID and could not be further
176 distinguished by LC-MS, there were 65 true identified metabolites and 1289 true annotated
177 metabolites (Table S2). 53 identified metabolites were present in both human urine and
178 MP-AU, while 10 metabolites were only present in human urine, and two were only present
179 in MP-AU (Fig. 2a). Of the 53 identified metabolites in common between the two media,
180 only orthophosphate and nicotinamide were more abundant in MP-AU compared to human
181 urine. The difference was statistically significant for orthophosphate ($P \leq 0.05$) but not for
182 nicotinamide. The remaining 51 metabolites were more abundant in human urine. There
183 was no statistical significance in the different average abundances of creatinine or oxalate
184 between human urine and MP-AU. The increased abundance in human urine compared to
185 MP-AU was statistically significant ($P \leq 0.05$) for six metabolites, highly significant ($P \leq 0.01$)
186 for 26 metabolites and very highly significant ($P \leq 0.001$) for 18 metabolites. We chose to
187 focus only on the identified metabolites, rather than annotated metabolites. The ratio of
188 metabolites in MP-AU relative to human urine is shown in Fig. 2b.

189 *Modifying MP-AU*

190 Metabolites were added to MP-AU based on their relative abundance in PHU samples over
191 MP-AU, or studies published in the literature. Where LC-MS identified metabolites that
192 were synthesized as by-products of another metabolite's degradation or synthesis, the by-
193 product was not included in the enhanced AU formulation. For example, LC-MS analysis
194 showed that L-kynurenine is present in PHU. L-kynurenine is a by-product of tryptophan
195 catabolism (van der Leek *et al.*, 2017) and therefore L-tryptophan was used as a supplement
196 instead of L-kynurenine. The majority of amino acids added were L-enantiomers, due to
197 their physiological relevance in protein synthesis (Suzuki *et al.*, 2021). There have also been
198 reports of endogenous D-amino acids eukaryotes, such as D-glutamate (Katane *et al.*, 2020),
199 D-cysteine (Roychaudhuri and Snyder, 2022) and D-serine (Anfora *et al.*, 2008; Cava *et al.*,
200 2011), hence these were also added. Although it was not in our LC-MS dataset, D-sorbitol is
201 listed on the Urine Metabolome Database with detected quantities in the urine of adults at
202 3.5-9.9 $\mu\text{mol mmol}^{-1}$ creatinine (Bouatra *et al.*, 2013) and was included as it is suggested to
203 be an important carbon source for UPEC strains in the urinary tract (Mann *et al.*, 2017). The
204 components were added to MP-AU at a final concentration of 0.5 mol L⁻¹, and this was
205 sufficient to support the growth of CFT073 and UTI89 (Fig. 3a). Both strains achieved the
206 same OD600 after 8 h in enhanced AU and the OD600 of CFT073 was the same as that in
207 PHU. Later experiments examined the viability of CFT073 and UTI89 when grown in
208 enhanced AU compared to LB medium, M9 minimal medium, MP-AU, and MP-AU
209 supplemented with peptone and yeast extract (Fig. S1a). The average numbers of CFT073
210 and UTI89, measured as colony forming units (CFU) mL⁻¹, do not increase during 8 h in MP-
211 AU (Fig. S1b). Iron is an important metal for the survival of UPEC strains in the urinary tract,
212 with UPEC strains encoding a number of proteins that acquire, scavenge, increase the

213 uptake of iron from urine. Sarigul's MP-AU does not include iron but Brooks and Keevil's
214 artificial urine formulation contains small amounts of iron (II) sulfate (Brooks and Keevil,
215 1997; Sarigul *et al.*, 2019). To assess iron levels in PHU, we used inductively coupled plasma
216 mass spectrometry (ICP-MS) to compare iron levels in PHU with enhanced AU supplemented
217 with iron (II) sulfate at 1 mmol L⁻¹. ICP-MS revealed that the levels of iron in PHU was
218 negligible, while the levels in our enhanced AU were sixty-fold higher (Fig. S2). As a result,
219 iron (II) sulfate was omitted from subsequent formulations.

220 *Transcriptomic analysis in EnAU*

221 Transcriptomics provides a global insight into how the bacterial cell responds to its
222 environment. Subtle changes in the nutrient content of the growth medium are reflected in
223 distinct patterns of gene expression. Moreover, if enhanced AU is to be used to study UPEC
224 *in vitro*, it is important to understand if key virulence genes are expressed to the same
225 extent. To determine whether this was the case, transcriptomic analysis was performed on
226 RNA extracted from CFT073 and UTI89 cultured in enhanced AU or PHU. Samples for RNA
227 extraction were taken during the mid-exponential phase to better capture the
228 transcriptomic profile during growth in either condition. In contrast to the original MP-AU
229 formulation where thousands of genes were affected, in this enhanced AU, 6.9% of the
230 CFT073 coding sequences (340 genes) and 3.8% of the UTI89 coding sequences (189 genes)
231 were significantly differentially expressed compared to PHU. There were 151 significant
232 upregulated genes in CFT073 in enhanced AU compared to PHU, and 189 significant
233 downregulated genes (Fig. 3b). In UTI89, there were 91 upregulated and 98 downregulated
234 genes, including the hypothetical protein-encoding gene *UTI89_RS29285* carried on the
235 UTI89 plasmid (Fig. 3c). The 50 most significant differentially expressed genes in CFT073 and
236 UTI89 are shown in Tables S3 and S4, respectively.

237 *Expression of virulence factors in EnAU*

238 Promisingly, a number of genes associated with virulence were similarly expressed (not
239 significantly up or downregulated) in CFT073 or UTI89 in EnAU and PHU. We examined
240 genes known to be associated with virulence, such as those encoding toxins, adhesins,
241 siderophores and iron uptake systems.

242 Almost half of all UPEC strains secrete the pore-forming toxin hemolysin (Nhu *et al.*, 2019).

243 Hemolysin is encoded for by *hlyA*, which is similarly expressed in CFT073 and UTI89 in EnAU
244 and PHU. Another toxin, cytotoxic necrotizing factor 1 or CNF1, is an important toxin
245 expressed by some UPEC strains, including UTI89, but it is not encoded for by the CFT073
246 genome (Smith *et al.*, 2008). Here, there was a similar level of expression of *cnf1* in UTI89 in
247 both EnAU and PHU. Unlike UTI89, CFT073 produces the serine protease autotransporter
248 toxins Pic and Sat. These genes (*pic* and *sat*, respectively) are similarly expressed in both
249 EnAU and in PHU. The colibactin genotoxin is expressed during UTI in humans, and is
250 associated with DNA damage in the urothelial cells in a mouse model of UTI (Chagneau *et*
251 *al.*, 2021). 17 CFT073 *clb* genes and 15 UTI89 *clb* genes, which encode colibactin, were
252 similarly expressed in EnAU and PHU.

253 Adherence to the uroepithelium through the expression of adhesins is a critical step in
254 uropathogenesis. Six genes in the type 1 fimbriae operon (*fimC*, *fimD*, *fimF*, *fimG*, *fimH* and
255 *fimI*) were significantly upregulated in CFT073 in EnAU compared to in PHU. In contrast, only
256 three type 1 fimbriae genes (*fimF*, *fimG* and *fimH*) in UTI89 were significantly upregulated in
257 EnAU compared to PHU. The adhesin FimH was significantly upregulated, 3-fold in CFT073
258 and 3.5-fold in UTI89 when cultured in EnAU compared with PHU.

259 Perhaps this is unsurprising, as Greene *et al.* found that culture in filtered human urine
260 induces the phase OFF phase of UTI89 *fimS* (Greene *et al.*, 2015). While *fim* operon

261 expression is upregulated in EnAU compared to PHU, this is still an advantage for the further
262 study of type 1 fimbriae expression and function under different conditions. The
263 pyelonephritis-associated pili (pap) or P fimbriae, thought to be associated with adhesion in
264 the kidney, are similarly expressed in CFT073 in EnAU and PHU. Of all the *pap* operon genes
265 in CFT073, only *papH_1* is significantly differentially expressed in EnAU relative to PHU (2.6-
266 fold increase). *CsgBA* are the minor and major subunits of the curli fibers associated with
267 adhesion and are similarly expressed in CFT073 in both EnAU and in PHU, however *csgC* is
268 significantly downregulated. In UTI89, the *csgBAC* operon is similarly expressed in both the
269 media. The S and F1C fimbriae are encoded for by the *sfa* and *foc* genes, which are also
270 similarly expressed by CFT073 in EnAU and in PHU.

271 Survival and growth in the urinary tract requires the uptake of iron from a nutritionally-poor
272 environment via iron-uptake systems and siderophores that are secreted by UPEC strains
273 (Frick-Cheng *et al.*, 2022). The *sitABCD* genes, which encode an iron/manganese ABC
274 transporter, are similarly expressed in CFT073 and UTI89 in EnAU and PHU, as well as the
275 genes encoding TonB-dependent heme receptors ChuA (*chuA*) and Hma (*C_RS11765*,
276 *UTI89_C2234*).

277 Siderophores aerobactin, enterobactin, salmochelin and yersiniabactin are encoded by
278 UPEC strains to bind to iron sequestered by the host, for example in hemoglobin (Frick-
279 Cheng *et al.*, 2022). Aerobactin genes *iucABCD* are similarly expressed in CFT073 in EnAU
280 and in PHU, so too is the gene encoding its receptor *iutA*. In CFT073 and UTI89, enterobactin
281 genes *entCEBAH*, *entD* and *entS*, *fepA* (encoding the enterobactin receptor), salmochelin
282 genes *iroBCDE* and *iroN* (encoding the salmochelin receptor) were similarly expressed in
283 EnAU and PHU. Of the yersiniabactin genes, only *ybtX*, which encodes the yersiniabactin-
284 associated zinc MSF transporter YbtX, is significantly upregulated in CFT073 in EnAU

285 compared to in PHU. The other yersiniabactin genes are similarly expressed. None of the
286 UTI89 *ybt* genes were significantly differentially expressed in EnAU compared to PHU.

287 *Suitability of enhanced AU to study other UPEC strains*

288 While CFT073 and UTI89 are prototypic model strains for UPEC study, there is great diversity
289 in the range of isolates associated with UTIs. A versatile artificial urine must be robust
290 enough to support the growth of a variety of strains. To determine the usefulness of our
291 enhanced AU, growth assays were performed on isolates taken from patients who had been
292 catheterized, and subsequently developed blood infections. The isolates were varied in
293 serotype but all from the B2 phylogroup that is strongly associated with UPEC infections.
294 Enhanced AU supported the growth of these clinical isolates demonstrating that it is useful
295 in supporting the growth of other UPEC strains, not just the prototypical laboratory strains
296 (Fig. 4).

ORIGINAL UNEDITED MANUSCRIPT

297 **Discussion**

298 Advances in formulation of artificial urine have meant that there are a number of different
299 formulations proposed in the literature or available commercially. There are many examples
300 of artificial urine facilitating research on UPEC in the past, with a number of studies using
301 the Brooks and Keevil artificial urine medium for different purposes. Examples include the
302 studying UPEC strains and other urinary pathogens (Juarez and Galván, 2018; Psotta *et al.*,
303 2023), studying ethanolamine metabolism during UPEC culture (Dadswell *et al.*, 2019),
304 examining the effect of probiotic *Lactobacillus* strains on biofilm formation (Carvalho *et al.*,
305 2021), and in investigating the use of metabolites to boost the effect of the broad-spectrum
306 antimicrobial nitrofurantoin (Aedo *et al.*, 2021). In addition to the Brooks and Keevil artificial
307 urine medium, commercially available artificial urine (LCTech GmbH) has been used in the to
308 study virulence mechanisms in CFT073 cultured in LB medium compared to artificial urine
309 (Sarshar *et al.*, 2022). The use of artificial urine in existing studies is evidence of its
310 importance. Some artificial urine formulations used to culture bacterial strains *in vitro*
311 contain components not normally present in healthy human urine. Here, we attempted to
312 modify MP-AU to better resemble PHU in terms of the ability to support growth of UPEC
313 strains and to induce a similar transcriptomic profile during growth. MP-AU described in the
314 literature was not suitable for the culture of UPEC strains CFT073 and UTI89 when peptone
315 and yeast extract were omitted. Peptone and yeast extract used in some artificial urine
316 formulations act as sources of amino acids, short peptides, trace elements and nucleic acids
317 that may be normally present in human urine (Brooks and Keevil, 1997). As the quantities of
318 components in commercially available reagents such as peptone and yeast extract are not
319 always available, our approach of supplementing MP-AU with specific quantities of amino
320 acids and metabolites aims to generate a more defined and reproducible medium. The

321 complexity of urine suggests that there are certain factors in the urine that allow for growth
322 and survival of those UPEC strains *in vitro*. As revealed by LC-MS, there were 65 identified
323 metabolites that varied in abundance between PHU and MP-AU. Unfortunately, LC-MS can
324 indicate relative abundances but cannot be used to precisely quantify the metabolites
325 present in a sample. Additionally, LC-MS cannot identify all of the metabolites present in a
326 sample. LC-MS was used here only to identify metabolites in PHU that could be used to
327 supplement MP-AU. The supplementation of MP-AU with amino acids and other
328 metabolites identified in PHU to generate the enhanced AU provides sources of carbon and
329 nitrogen that are required for the growth of UPEC strains. Nutritional selection and UPEC
330 metabolism is reviewed elsewhere (Chan and Lewis, 2022). It is worth noting that these
331 studies were all performed on filtered urine. Filter sterilization may result in the loss of
332 components that contribute to bacterial growth and/or gene expression *in vivo*.
333 Furthermore, *in vivo*, there is constant voiding and replenishing of urine in the bladder,
334 whereas in our *in vitro* experiments, the medium is not replenished. Nevertheless, similar
335 levels of transcription between the two media suggests that EnAU does in fact mimic
336 conditions of PHU and we have generated an artificial urine that is consistent for growth of
337 multiple UPEC strains for studying expression of virulence genes *in vitro*.

338 **Acknowledgements**

339 The authors thank Glasgow Polyomics, Dr Lorna Eades at the University of Edinburgh, and
340 Professor Thomas Evans, Dr Cosmika Goswami and Dr Stephen Fox at the University of
341 Glasgow for their help in this work. For the purpose of open access, the authors have
342 applied a Creative Commons Attribution (CC BY) license to any Author Accepted Manuscript
343 version arising from this submission.

344 **Funding**

345 PTR was funded by a University of Glasgow PhD studentship in collaboration with GSK. NOB
346 was supported by the Biotechnology and Biological Sciences Research Council
347 [BB/R006539/1]. GRD and AJR were supported by the Biotechnology and Biological Sciences
348 Research Council [BB/W015781/1]. AJR was also supported by the Medical Research Council
349 [MR/V011499/1].

350 **Conflict of interest**

351 No conflict of interest declared.

352 **Data availability**

353 Raw sequencing data have been deposited in the European Nucleotide Archive under the
354 project accession number PRJEB55151.

355 **References**

- 356 Aedo, S.J., Tang, J.C., and Brynildsen, M.P. (2021) Metabolites potentiate nitrofurans in
357 nongrowing *Escherichia coli*. *Antimicrobial Agents and Chemotherapy* **65**.
- 358 Anfora, A.T., Halladin, D.K., Haugen, B.J., and Welch, R.A. (2008) Uropathogenic *Escherichia*
359 *coli* CFT073 is adapted to acetatogenic growth but does not require acetate during murine
360 urinary tract infection. *Infection and Immunity* **76**: 5760-5767.
- 361 Bateman, A., Martin, M.-J., Orchard, S., Magrane, M., Agivetova, R., Ahmad, S. *et al.* (2021)
362 UniProt: the universal protein knowledgebase in 2021. *Nucleic Acids Research* **49**: D480-
363 D489.
- 364 Bouatra, S., Aziat, F., Mandal, R., Guo, A.C., Wilson, M.R., Knox, C. *et al.* (2013) The human
365 urine metabolome. *PLoS One* **8**: e73076.
- 366 Brooks, T., and Keevil, C.W. (1997) A simple artificial urine for the growth of urinary
367 pathogens. *Letters in Applied Microbiology* **24**: 203-206.
- 368 Carvalho, F.M., Mergulhao, F.J.M., and Gomes, L.C. (2021) Using Lactobacilli to fight
369 *Escherichia coli* and *Staphylococcus aureus* biofilms on urinary tract devices. *Antibiotics-*
370 *Basel* **10**.
- 371 Cava, F., Lam, H., de Pedro, M.A., and Waldor, M.K. (2011) Emerging knowledge of
372 regulatory roles of D-amino acids in bacteria. *Cell Mol Life Sci* **68**: 817-831.
- 373 Chagneau, C.V., Massip, C., Bossuet-Greif, N., Fremez, C., Motta, J.-P., Shima, A. *et al.* (2021)
374 Uropathogenic *E. coli* induces DNA damage in the bladder. *Plos Pathogens* **17**.
- 375 Chan, C.C.Y., and Lewis, I.A. (2022) Role of metabolism in uropathogenic *Escherichia coli*.
376 *Trends in Microbiology* **30**: 1174-1204.
- 377 Chutipongtanate, S., and Thongboonkerd, V. (2010) Systematic comparisons of artificial
378 urine formulas for *in vitro* cellular study. *Analytical Biochemistry* **402**: 110-112.

379 Dadswell, K., Creagh, S., McCullagh, E., Liang, M., Brown, I.R., Warren, M.J. *et al.* (2019)
380 Bacterial microcompartment-mediated ethanolamine metabolism in *Escherichia coli* urinary
381 tract infection. *Infection and Immunity* **87**.

382 Frick-Cheng, A.E., Sintsova, A., Smith, S.N., Pirani, A., Snitkin, E.S., and Mobley, H.L.T. (2022)
383 Ferric citrate uptake is a virulence factor in uropathogenic *Escherichia coli*. *Mbio* **13**.

384 Gloaguen, Y., Morton, F., Daly, R., Gurden, R., Rogers, S., Wandy, J. *et al.* (2017) PiMP my
385 metabolome: an integrated, web-based tool for LC-MS metabolomics data. *Bioinformatics*
386 **33**: 4007-4009.

387 Goswami, C., Fox, S., Holden, M., Connor, M., Leanord, A., and Evans, T.J. (2018) Genetic
388 analysis of invasive *Escherichia coli* in Scotland reveals determinants of healthcare-
389 associated versus community-acquired infections. *Microbial Genomics* **4**.

390 Greene, S.E., Hibbing, M.E., Janetka, J., Chen, S.L., and Hultgren, S.J. (2015) Human urine
391 decreases function and expression of type 1 pili in uropathogenic *Escherichia coli*. *Mbio* **6**.

392 Hultgren, S.J., Schwan, W.R., Schaeffer, A.J., and Duncan, J.L. (1986) Regulation of
393 production of type 1 pili among urinary tract isolates of *Escherichia coli*. *Infection and*
394 *Immunity* **54**: 613-620.

395 Juarez, G.E., and Galván, E.M. (2018) Role of nutrient limitation in the competition between
396 uropathogenic strains of *Klebsiella pneumoniae* and *Escherichia coli* in mixed biofilms.
397 *Biofouling* **34**: 287-298.

398 Katane, M., Nakasako, K., Yako, K., Saitoh, Y., Sekine, M., and Homma, H. (2020)
399 Identification of an L-serine/L-threonine dehydratase with glutamate racemase activity in
400 mammals. *Biochemical Journal* **477**: 4221-4241.

401 Mann, R., Mediati, D.G., Duggin, I.G., Harry, E.J., and Bottomley, A.L. (2017) Metabolic
402 adaptations of uropathogenic *E. coli* in the urinary tract. *Frontiers in Cellular and Infection*
403 *Microbiology* **7**.

404 Mobley, H.L.T., Green, D.M., Trifillis, A.L., Johnson, D.E., Chippendale, G.R., Lockatell, C.V. *et*
405 *al.* (1990) Pyelonephritogenic *Escherichia coli* and killing of cultured human renal proximal
406 tubular epithelial cells - role of hemolysin in some strains. *Infection and Immunity* **58**: 1281-
407 1289.

408 Nhu, N.T.K., Phan, M.-D., Forde, B.M., Murthy, A.M.V., Peters, K.M., Day, C.J. *et al.* (2019)
409 Complex multilevel control of hemolysin production by uropathogenic *Escherichia coli*. *Mbio*
410 **10**.

411 Psotta, C., Nilsson, E.J., Sjöberg, T., and Falk, M. (2023) Bacteria-infected artificial urine
412 characterization based on a combined approach using an electronic tongue complemented
413 with ¹H-NMR and flow cytometry. *Biosensors-Basel* **13**.

414 Roychaudhuri, R., and Snyder, S.H. (2022) Mammalian D-cysteine: A novel regulator of
415 neural progenitor cell proliferation. *Bioessays*.

416 Sarigul, N., Korkmaz, F., and Kurultak, I. (2019) A new artificial urine protocol to better
417 imitate human urine. *Scientific Reports* **9**.

418 Sarshar, M., Scribano, D., Limongi, D., Zagaglia, C., Palamara, A.T., and Ambrosi, C. (2022)
419 Adaptive strategies of uropathogenic *Escherichia coli* CFT073: from growth in lab media to
420 virulence during host cell adhesion. *International microbiology : the official journal of the*
421 *Spanish Society for Microbiology*.

422 Smith, Y.C., Rasmussen, S.B., Grande, K.K., Conran, R.M., and O'Brien, A.D. (2008) Hemolysin
423 of uropathogenic *Escherichia coli* evokes extensive shedding of the uroepithelium and

424 hemorrhage in bladder tissue within the first 24 hours after intraurethral inoculation of
425 mice. *Infection and Immunity* **76**: 2978-2990.

426 Suzuki, M., Sujino, T., Chiba, S., Harada, Y., Goto, M., Takahashi, R. *et al.* (2021) Host-
427 microbe cross-talk governs amino acid chirality to regulate survival and differentiation of B
428 cells. *Science Advances* **7**.

429 van der Leek, A.P., Yanishevsky, Y., and Kozyrskyj, A.L. (2017) The kynurenine pathway as a
430 novel link between allergy and the gut microbiome. *Frontiers in Immunology* **8**.

431

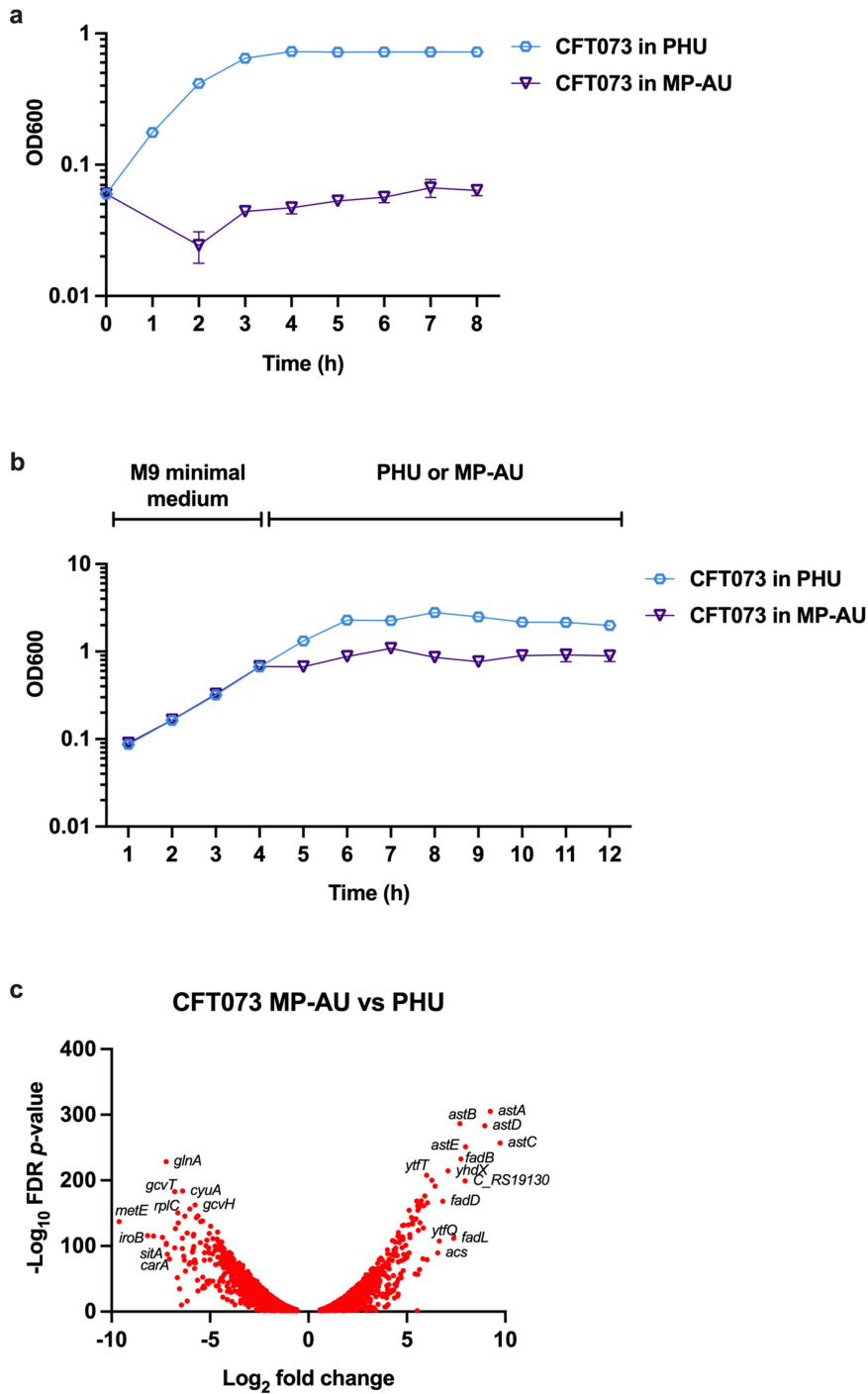
ORIGINAL UNEDITED MANUSCRIPT

432 **Author contributions**

433 Patricia Rimbi (Formal analysis, Investigation, Methodology, Visualization, Writing – original
434 draft, Writing – review & editing) Nicky O’Boyle (Investigation, Methodology, Writing –
435 review & editing), Gillian R. Douce (Conceptualization, Funding acquisition, Methodology,
436 Project administration Supervision), Mariagrazia Pizza (Funding acquisition, Supervision),
437 Roberto Rosini (Supervision), and Andrew J. Roe (Conceptualization, Methodology, Project
438 administration, Supervision, Writing – review & editing).

439

ORIGINAL UNEDITED MANUSCRIPT



441

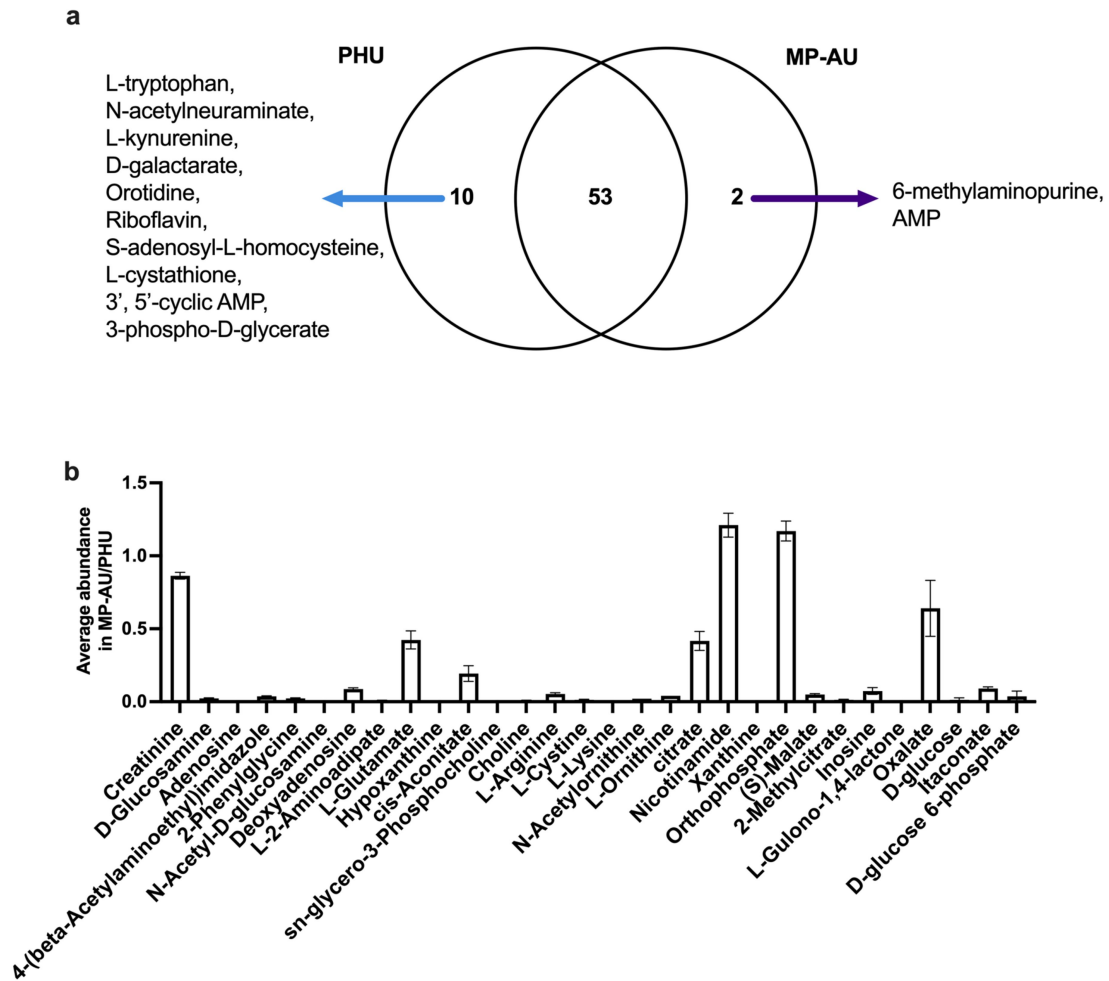
442 Fig 1. Assessing the suitability of multi-purpose artificial urine for *in vitro* culture of

443 uropathogenic *E. coli* strains. a) Growth profile of wild-type CFT073 when overnight

444 cultures were inoculated into pre-warmed filtered pooled human urine (PHU, blue

445 hexagons) or multi-purpose artificial urine (MP-AU, purple triangles). Error bars represent
446 the standard error of the mean of three biological replicates. **b) Growth profile of wild-type**
447 CFT073 when overnight cultures were inoculated into pre-warmed M9 minimal medium and
448 after 4 h, cultures were pelleted by centrifugation and resuspended in PHU (blue hexagons)
449 or MP-AU (purple triangles). Error bars represent the standard error of the mean of three
450 biological replicates. **c) Transcriptomic profile of wild-type CFT073 when grown in PHU and**
451 MP-AU. Volcano plot represents significant differentially expressed genes in MP-AU relative
452 to PHU. FDR $P \leq 0.05$, fold change ≥ 1.5 or ≤ -1.5 .
453

ORIGINAL UNEDITED MANUSCRIPT

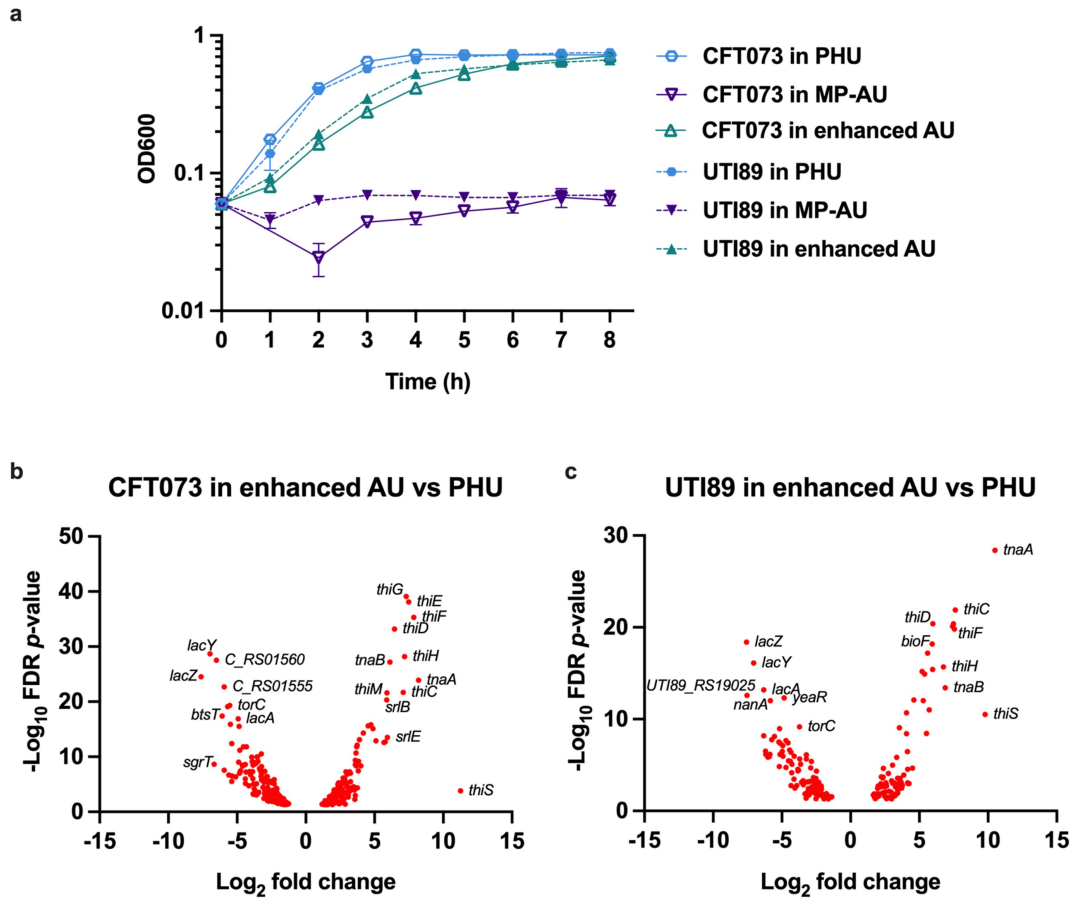


455

456 **Fig 2. Determining the metabolites present in pooled human urine and multi-purpose**
 457 **artificial urine by liquid chromatography mass spectrometry. a)** Venn diagram displaying
 458 the distribution of identified metabolites between pooled human urine (PHU) and multi-
 459 purpose artificial urine (MP-AU). **b)** The ratio of average abundance of identified
 460 metabolites in MP-AU relative to PHU. Metabolites with a ratio of average abundance of
 461 zero are excluded. Error bars represent the standard error of the mean of three technical
 462 replicates.

463

464



466

467 **Fig 3. Growth and transcriptomic profiles of model UPEC strains in enhanced AU vs PHU**468 **and MP-AU. a)** Growth profile of wild-type CFT073 and UTI89 when grown in pooled human

469 urine (PHU, blue hexagons), multi-purpose artificial urine (MP-AU, purple triangles) or

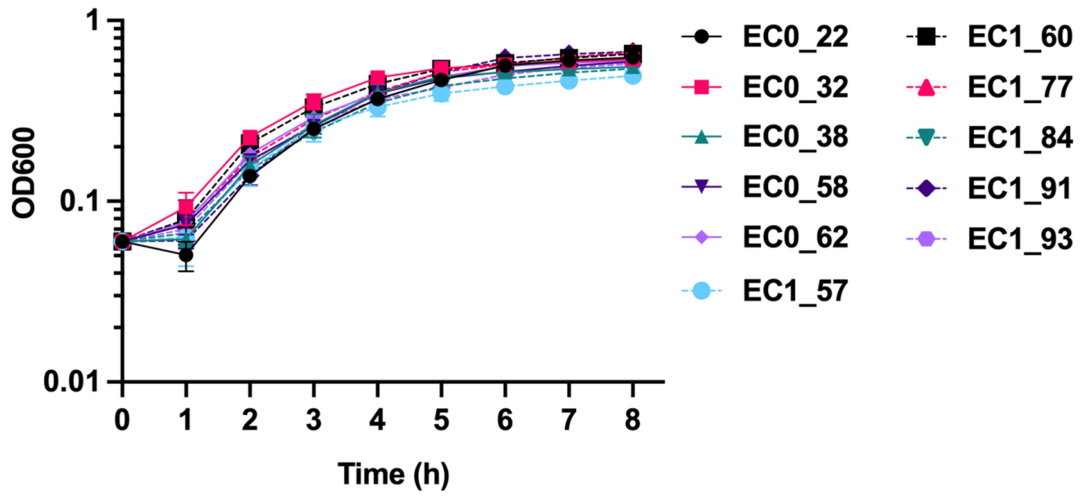
470 enhanced artificial urine (enhanced AU, green triangles). Error bars represent the standard

471 error of the mean of three biological replicates. **b and c)** Transcriptomic profile of CFT073

472 and UTI89 when grown in enhanced AU or PHU. Volcano plots represent significant

473 differentially expressed genes in enhanced AU relative to PHU. FDR $P \leq 0.05$, fold change474 ≥ 1.5 or ≤ -1.5 . Three biological replicates were performed.

475



477

478 **Fig 4. Growth of non-model UPEC strains in enhanced AU.** Growth profile of bacteremia
 479 isolates when grown in enhanced artificial urine. Error bars represent the standard error of
 480 the mean of three biological replicates.

481

ORIGINAL UNEDITED MANUSCRIPT

482

483 **Table 1.** Strains used in this study.

Name	Description	Phylogroup	Serotype	Reference
CFT073	Uropathogenic <i>E. coli</i> strain CFT073	B2	O6:H1	(Mobley <i>et al.</i> , 1990)
UTI89	Uropathogenic <i>E. coli</i> strain UTI89		O18:H7	(Hultgren <i>et al.</i> , 1986)
ECO_22	<i>E. coli</i> isolate ECO_22		O6:H1	(Goswami <i>et al.</i> , 2018)
ECO_32	<i>E. coli</i> isolate ECO_32		O1:H7	
ECO_38	<i>E. coli</i> isolate ECO_38		O25:H4	
ECO_58	<i>E. coli</i> isolate ECO_58		O18:H7	
ECO_62	<i>E. coli</i> isolate ECO_62		O2:H7	
EC1_57	<i>E. coli</i> isolate EC1_57		O18:H31	
EC1_60	<i>E. coli</i> isolate EC1_60		O22:H1	
EC1_77	<i>E. coli</i> isolate EC1_77		O16:H5	
EC1_84	<i>E. coli</i> isolate EC1_84		O4:H1	
EC1_91	<i>E. coli</i> isolate EC1_91		O18:H1	
EC1_93	<i>E. coli</i> isolate EC1_93		O6:H31	

484

485

486

487

488 **Table 2.** MP-AU components. The desired volume was made up with distilled deionized
489 water.

Component	Concentration in MP-AU	Supplier
Sodium sulfate decahydrate	11.965 mmol L ⁻¹	Sigma-Aldrich
Trisodium citrate	2.450 mmol L ⁻¹	Sigma-Aldrich
Creatinine	7.791 mmol L ⁻¹	Sigma-Aldrich
Urea	249.750 mmol L ⁻¹	Fisher Scientific
Uric acid	0.25 g L ⁻¹	Sigma-Aldrich
Potassium chloride	30.953 mmol L ⁻¹	Sigma-Aldrich
Sodium chloride	30.953 mmol L ⁻¹	Sigma-Aldrich
Calcium chloride	1.663 mmol L ⁻¹	Sigma-Aldrich
Ammonium chloride	23.667 mmol L ⁻¹	Sigma-Aldrich
Potassium oxalate monohydrate	0.190 mmol L ⁻¹	Sigma-Aldrich
Magnesium sulfate heptahydrate	4.389 mmol L ⁻¹	Sigma-Aldrich
Sodium phosphate monobasic dihydrate	18.667 mmol L ⁻¹	Sigma-Aldrich
Sodium phosphate dibasic dihydrate	4.667 mmol L ⁻¹	Sigma-Aldrich

490

491

492